

## The Interaction of Hydrazine with Polycrystalline Iridium Foil<sup>1</sup>

BERNARD J. WOOD AND HENRY WISE

*Solid State Catalysis Laboratory, Stanford Research Institute,  
Menlo Park, California 94025*

Received March 11, 1975

During the room temperature decomposition of hydrazine on a polycrystalline iridium foil, a number of surface adsorbates are formed. Temperature programmed desorption spectroscopy reveals that these adspecies include several distinct states of hydrogen and of nitrogen adatoms, in addition to a surface free radical that leads to ammonia by reaction with hydrogen adatoms. The relative population densities of the surface species change with increasing exposure to hydrazine. The initially high catalytic activity of the surface is affected by the surface density of nitrogen adatoms in the strongly bound  $\beta$ -state.

### 1. INTRODUCTION

The decomposition of hydrazine is catalyzed by a number of transition-group metals to give  $N_2$ ,  $H_2$ , and  $NH_3$ . Studies of the decomposition reaction on films of tungsten (1) and of molybdenum (2), and on alumina-supported iridium (3,4), suggest that an initial step in the catalytic process is dissociative adsorption of the hydrazine molecules. The species present on the surface include adatoms of nitrogen and of hydrogen, in addition to  $NH_2$  radicals. The hydrogen adatoms are highly mobile, and they may react with one another to give molecular hydrogen or with  $NH_2$  radicals to give ammonia. The  $NH_2$  radicals also may dissociate further on the surface until only chemisorbed nitrogen and hydrogen remain.

Surface studies of the states of nitrogen and hydrogen adatoms on Ir were carried out by Mimeault and Hansen (5,6). Dissociative chemisorption of nitrogen involves a considerable energy barrier in the case of Ir. Consequently, these investigators could dose a clean iridium wire with nitrogen adatoms only by exposure to gaseous ni-

trogen atoms produced by thermal dissociation of molecular nitrogen. They suggested the chemisorbed nitrogen to be strongly bound to the iridium with an energy of approximately 60 kcal/mole.

On the basis of this information, it seems likely that chemisorbed nitrogen or hydrogen, produced on the iridium catalyst during decomposition of hydrazine, may be bound strongly enough to remain on the surface. If these adatoms preempt sites on which dissociative adsorption of hydrazine can occur, they would tend to mitigate the activity of the catalyst.

The object of our study was to identify specific adsorbed species that might interfere with the hydrazine decomposition activity of an iridium surface. Our approach was to examine the catalytic characteristics of iridium for hydrazine decomposition under clean surface conditions and to follow the populations of various adstates on the surface.

### 2. EXPERIMENTAL DETAILS

To provide the capability for carrying out surface adsorption and reaction measurements on atomically clean surfaces, we used an ultrahigh vacuum (uhv) system. The reactor (Fig. 1), fabricated

<sup>1</sup> Support of this research by the Air Force Office of Scientific Research is gratefully acknowledged.

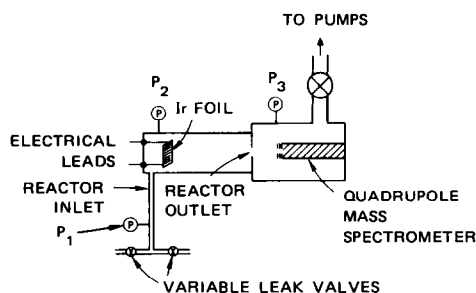


FIG. 1. Schematic diagram of apparatus; (P) ion gages.

from type 304 stainless steel tubing, had a 3.7-cm inside diameter and was 8.5-cm long. It was equipped with four side arms with standard uhv flange fittings through which connections were made to the pumping system, to a quadrupole mass spectrometer, to gas inlet valves, and to a fixture to support the iridium catalyst. The total volume of the chamber and side arms was approximately 270 cm<sup>3</sup>. The catalyst was a narrow ribbon ( $0.0046 \times 0.071 \times 6.9$  cm) of 99.9+ % pure iridium foil suspended in a catenary loop from glass-shielded tungsten lead-throughs with stainless steel screw connectors. The lead-throughs and connectors were relatively massive, and they experienced little temperature rise when the ribbon was heated by passage of an electric current. Catalyst temperature as a function of heating current was determined by means of an Infrascopes radiation thermometer, and, in selected experiments, by a 0.003-in. Chromel-Alumel thermocouple spot-welded to the center of the ribbon. A blank experiment, for which the iridium ribbon was removed from the reactor, demonstrated that the walls had negligible activity for hydrazine decomposition at room temperature.

Hydrazine vapor and other gases were admitted to the reactor through appropriate uhv valves. Unreacted hydrazine and the reaction products flowed out of the reactor through a 0.635-cm diameter circular orifice in a 0.204-cm thick copper plate, directly into the ionization chamber

of a quadrupole mass spectrometer (QMS). From the pressures measured with ion gages in the reactor,  $P_R$ , and in the QMS chamber,  $P_A$ , and the calculated value of the conductance,  $F$ , of the exit orifice (short pipe approximation) (7), the mass flow rate,  $Q_o$ , of effluent could be determined:

$$Q_o = F(P_R - P_A). \quad (1)$$

By means of such data, the QMS was calibrated using O<sub>2</sub>, N<sub>2</sub>, H<sub>2</sub>, and NH<sub>3</sub> to give a measure of the mass flow rate of the respective gases out of the reactor in terms of the heights of their major peaks. Hence, the QMS data indicated the composition of the reaction products and, in addition, their rate of formation in the reactor. Peak heights at amu 17 were used to measure NH<sub>3</sub> only after subtracting the contributions to this peak from hydrazine (amu 32) and water (amu 18). Peaks at amu 14 and at amu 28 were used to monitor nitrogen.

The vacuum system was pumped by ion-getter and titanium sublimation pumps. Base pressures in the region of  $6 \times 10^{-10}$  Torr were obtained after brief bakeouts at about 200°C. Experiments were carried out at reactor pressures  $< 10^{-6}$  Torr; hence, mass transport was exclusively by molecular flow, and gas-phase collisions between molecules during their sojourn in the reactor were negligible. Under molecular flow conditions the residence time of a gaseous molecule in the reactor may be meaningfully expressed in terms of the average number of collisions the molecule makes with the surfaces before it "sees" the exit orifice and leaves the reactor. To a first approximation (8), the value of this collision number for the catalyst,  $\sigma$ , may be defined as the ratio of the catalyst surface area  $A_s$  to the exit orifice equivalent cross section  $A_e$ . In our case  $\sigma = 4$ .

Two types of experiments were carried out. In the first, the catalyst surface was initially cleaned by heating to about 1500 K under vacuum ( $P < 10^{-9}$  Torr); sub-

sequently, it was cooled to room temperature and then dosed by exposure to hydrazine vapor. After a fixed period of time, the hydrazine flow through the reactor was cut off. Subsequently, the iridium ribbon was rapidly heated at a prescribed nearly linear rate of temperature rise to desorb species remaining adsorbed on the surface from the preceding dosing period. In such a transient experiment, the efflux of gases through the outlet at any instant is given by the sum of the rates of desorption,  $\Sigma(-dn/dt)$ , less a correction term, which depends on the volume  $V$  of the reactor and the conductance  $F$  of the exit orifice (9):

$$Q_o = \Sigma(-dn/dt) - (V/F) (dQ_o/dt). \quad (2)$$

By suitable calibration, the temperature at which the maximum rate of desorption of

each surface species occurs may be determined from the QMS data taken as a function of time. The quotient  $V/F$  represents the characteristic pumping time (9),  $\tau$ , of the system. In our case,  $\tau = 0.097$  sec.

At the temperatures corresponding to maxima in the desorption spectra (Fig. 2),  $dQ_o/dt = 0$ . In view of the small value of  $\tau$ , the observed values of  $Q_o$  at these temperatures closely approximate the actual maximum desorption rates of the individual binding states of the adsorbates. In the case of second order desorption kinetics for hydrogen and nitrogen (10), we may apply a rate law of the form

$$-(dn/dt) = An^2 \exp(-E/RT), \quad (3)$$

where  $A$  is the preexponential constant,  $n$  is the number density of adatoms ( $\text{cm}^{-2}$ ),  $E$  is the activation energy for desorption

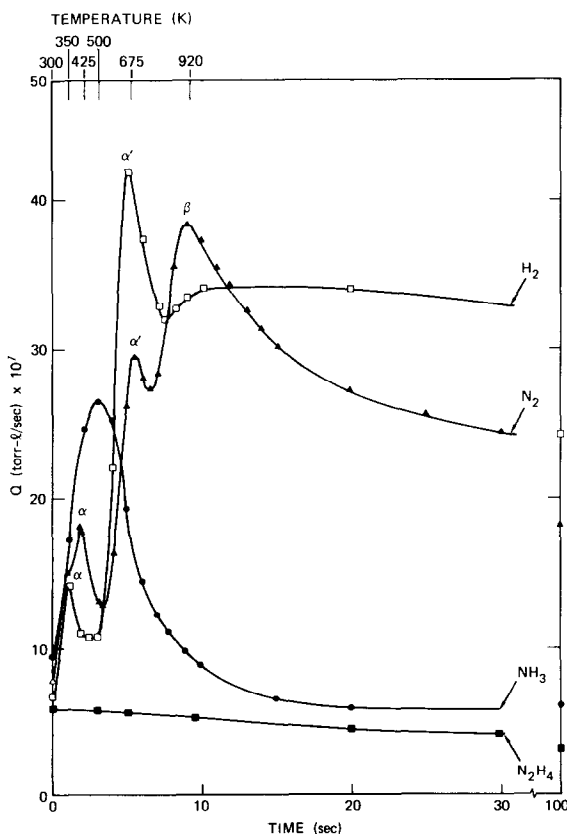


FIG. 2. Desorption spectra from hydrazine-dosed iridium. Heating rate  $\beta = 78 \text{ K sec}^{-1}$ . Dosed at 300 K with exposure of  $\sim 50$  Langmuirs.

(cal/mole),  $R$  is the gas constant, and  $T$  is the surface temperature (K). At the temperature ( $T_m$ ) of maximum desorption rate, the derivative with respect to time of Eq. (3) may be set equal to zero, so that

$$E/RT_m^2 = (2An_m/\beta) \exp(-E/RT_m), \quad (4)$$

where  $\beta = dT/dt$ , the linear heating rate of the surface (in our experiments,  $75 < \beta < 335 \text{ sec}^{-1}$ ). Equation (4) provides an analytical relationship between  $\beta$  and  $T_m$ . By rearrangement of Eq. (4) into slope-intercept form with respect to  $\beta$  and  $T_m$ ,

$$\ln(\beta/T_m^2) = \ln(2RA n_m/E) - E/RT_m, \quad (5)$$

we note that measurements of  $T_m$  for various heating rates permit us to evaluate  $E$  from the slope of a plot of  $\ln(\beta/T_m^2)$  versus  $1/T_m$ . The intercept of this plot gives the value of the product  $A \cdot n_m$ . Such an analysis is valid when the initial surface coverage by the adsorbate is held constant (11).

To obtain the value of the preexponential constant  $A$ , it is necessary to know the value of  $n_m$ . In principle, the value of this parameter can be obtained by summing the area under the desorption peak. The desorption peaks obtained in our experiments, however, exhibited pronounced tailing, which prevented us from making a meaningful measurement of  $n_m$ , since the area under the peak is a sensitive function of the assumed base line. In contrast, measurements of peak heights, proportional to  $-(dn/dt)_m$ , are considerably less sensitive to the selection of a diagonal base line. An expression derived from Eqs. (3) and (4),

$$n_m = (2RT_m^2/E\beta)(-dn/dt)_m, \quad (6)$$

permits calculation of  $n_m$  from a knowledge of  $E$  and from measurement of  $-(dn/dt)_m$ , and separation of the value of the preexponential constant  $A$  from the product  $A \cdot n_m$ .

In the second type of experiment, a constant flow of hydrazine vapor was bled into

the reactor while the composition and flow rate of products in the reactor effluent were recorded by the QMS as a function of catalyst temperature. In such a steady-state situation, the mass flow of reactant into the reactor,  $Q_i$ , is related to the total mass flow out of the reactor,  $Q_o$ , by the equation:

$$Q_o = (Q_i - Q_R) + \Sigma Q_P, \quad (7)$$

where  $Q_R$  is the rate of decomposition of the reactant on the catalyst and  $\Sigma Q_P$  is the sum of the rates of formation of products. Consequently, under these conditions the rate of efflux of each product observed by the mass spectrometer is a direct measure of its rate of formation on the catalyst surface.

The hydrazine used in our experiments was anhydrous technical grade (Olin-Mathieson). Water was removed by exposing the liquid  $N_2H_4$  to calcium hydride or Linde 5A molecular sieve. Noncondensable gas was removed by a cycle of freezing, pumping, and thawing. Then the vapor was transferred at room temperature into an evacuated 2-liter glass storage bulb. Hydrogen was purified by diffusion through a palladium thimble; ammonia was CP grade obtained from The Matheson Co.

### 3. RESULTS

Typical desorption spectra obtained from the hydrazine-dosed iridium ribbon are shown in Figs. 2 and 3. Qualitatively, these spectra suggest that the dosed surface harbors nitrogen in three distinct binding states ( $\alpha$ ,  $\alpha'$ , and  $\beta$ ), hydrogen in two states ( $\alpha$  and  $\alpha'$ ), and molecularly adsorbed ammonia (Fig. 2).

The long tails on the  $\beta$ -hydrogen and  $\beta$ -nitrogen peaks were most pronounced after exposure of the ribbon to larger doses of hydrazine. Shorter exposures resulted in less tailing (Fig. 3). Most likely the sustained high fluxes of nitrogen are a consequence of continued decomposition on

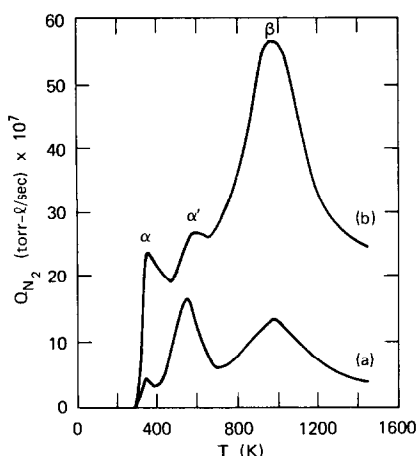


FIG. 3. Desorption spectra of nitrogen from hydrazine-dosed iridium. Heating rate  $\beta = 270 \text{ K sec}^{-1}$ . Dosed at 300 K with exposure of: (a) 7 Langmuirs ( $P \sim 5 \times 10^{-8}$  Torr); (b) 300 Langmuirs ( $P \sim 10^{-6}$  Torr).

the hot iridium surface of hydrazine that originates from an adsorbate on the wall of the reactor. This hydrazine was adsorbed on the wall during the dosing period in a weakly bound (perhaps physisorbed) state at a coverage proportional to the exposure.

For steady-state experiments in the constant-collision-number reactor, it is convenient to discuss changes in activity of the catalyst in terms of the mole fraction of hydrazine in the reactor effluent; the larger this value, the lower the catalytic activity of the iridium. We found that the room temperature initial activity of iridium,

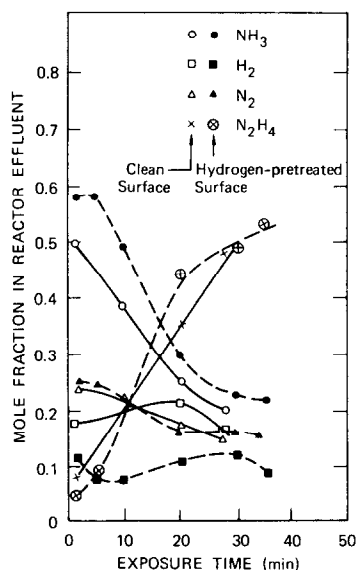
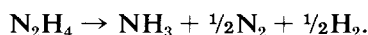


FIG. 4. Product distribution following exposure of iridium to hydrazine at  $P \sim 10^{-6}$  Torr at 300 K. Open symbols: freshly cleaned ribbon; filled symbols: ribbon pretreated by exposure to  $\text{H}_2$ .

freshly cleaned by heating to 1500 K, was high (Fig. 4). On initial introduction of hydrazine, the mole ratios of the products of decomposition are nearly in accordance with the stoichiometry



With continued exposure, the fraction of unreacted hydrazine increases slowly at the expense of the reaction products. However, the initial stoichiometry is

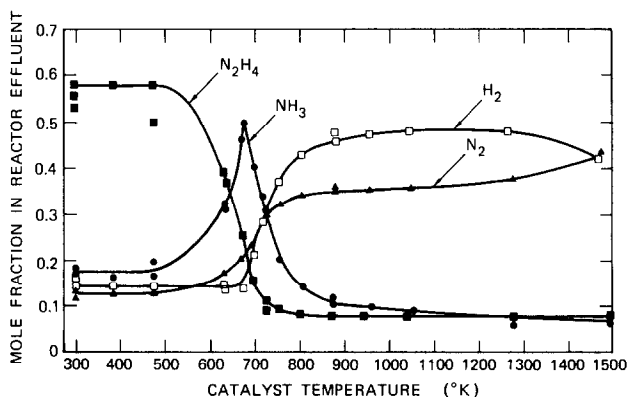


FIG. 5. Steady-state decomposition products of hydrazine on iridium as a function of catalyst temperature.  $P$  reactor:  $\sim 10^{-6}$  Torr.

approximated under steady-state conditions from room temperature up to about 500 K (Fig. 5). At higher temperatures, the product distribution changes to correspond more nearly to the stoichiometry



Desorption spectra and steady-state decomposition data were obtained also for ammonia as a reactant, under similar conditions. The desorption spectra (Fig. 6) exhibit superimposed nitrogen and hydrogen peaks as primary features. The maxima of these peaks appear at a temperature close to that at which the  $\alpha'$  peaks occur on desorption from hydrazine-dosed iridium. Under steady-state conditions (Fig. 7), ammonia is quite stable at temperatures up to  $T > 600$  K, where rapid decomposition commences. The observed

diminution in the steady-state rate of decomposition of ammonia at ribbon temperatures greater than 750 K can be attributed to a diminution in the surface residence time of the ammonia molecules in this temperature regime.

#### 4. DISCUSSION

A common feature of the desorption spectra obtained from hydrazine-dosed and from ammonia-dosed iridium ribbons is the appearance of hydrogen and nitrogen peaks at temperatures close to 600 K. A striking difference in these spectra is the diminutive amplitude of the molecular ammonia peak recovered from the ammonia-dosed ribbon relative to that obtained from the hydrazine-dosed ribbon (cf. Figs. 6 and 2). The steady-state experiments with these reactants show that, on a clean iridium surface, hydrazine decomposes rapidly at room temperature, whereas ammonia is quite stable (cf. Figs. 4 and 7). However, the rate of ammonia decomposition increases as the temperature of the surface approaches 600 K (Fig. 7). For each reactant, major products of decomposition are nitrogen and hydrogen.

The simultaneous appearance of hydrogen and nitrogen peaks at about 600 K in the desorption spectra suggests that they arise from a single surface reaction step that involves a common intermediate. Adsorbed molecular ammonia is an obvious choice for this intermediate. Indeed, Contour and Pannetier (3) interpret an ir band obtained from hydrazine adsorbed on iridium to arise from chemisorbed ammonia. However, for the interaction of  $\text{NH}_3$  with Ir, our desorption spectrum indicates that molecular ammonia is bound to the surface with sufficient strength that it prefers decomposition to desorption as the temperature of the metal is raised (Fig. 6). Hence, the ammonia desorbed from the hydrazine-dosed ribbon at room temperature must come from a surface reaction between hydrazine dissociation products,

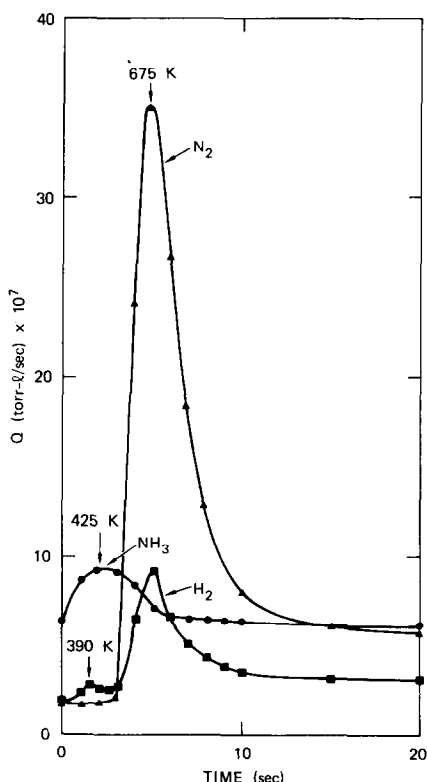


FIG. 6. Desorption spectra from ammonia-dosed iridium. Heating rate  $\beta = 78 \text{ K sec}^{-1}$ . Dosed at 300 K with exposure of  $\sim 50$  Langmuirs.

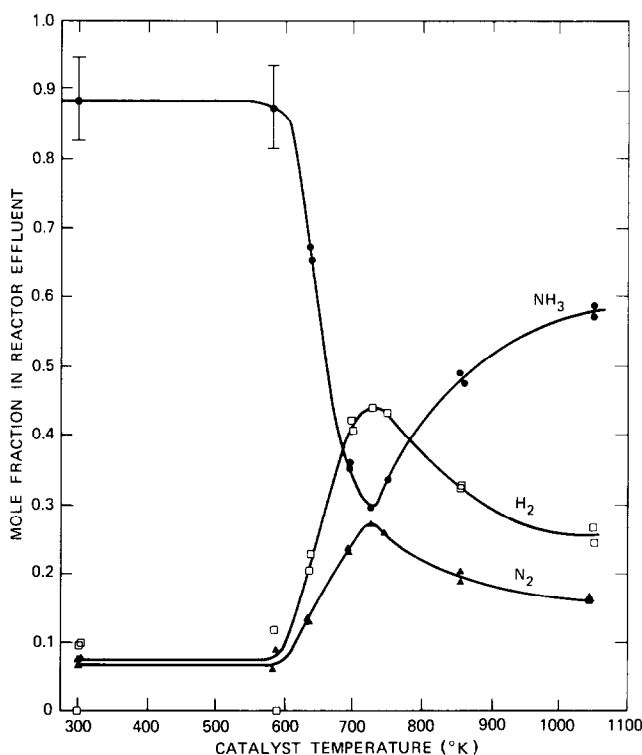


FIG. 7. Steady-state decomposition products of ammonia on iridium as a function of temperature. *P* reactor:  $\sim 5 \times 10^{-7}$  Torr.

such as the reaction of  $\text{NH}_2^*$  radicals with hydrogen adatoms,  $\text{H}^*$ . (Throughout our text, the asterisk indicates adsorbed species.) A number of investigators (1-4) have reported that dissociative adsorption of  $\text{N}_2\text{H}_4$  occurs on iridium and on other metals. The occurrence of such a reactive chemisorption step for  $\text{N}_2\text{H}_4$ , but not for  $\text{NH}_3$ , is consistent with the greater thermodynamic stability of  $\text{NH}_3$ ; the energy of the  $\text{H}-\text{NH}_2$  bond (12) is 110 kcal/mole, while that of the  $\text{H}_2\text{N}-\text{NH}_2$  bond (13) is 71 kcal/mole.

However, there is considerable evidence, based on studies of the decomposition of  $^{15}\text{N}$ -labeled hydrazine on Pyrex (14),  $\text{MgO}$ -supported iron (15), and alumina-supported iridium in an aqueous medium (16), that the  $\text{N}-\text{N}$  bond is not broken in the process of  $\text{N}_2$  formation. Consequently, it seems likely that a surface intermediate in which the  $\text{N}-\text{N}$  bond

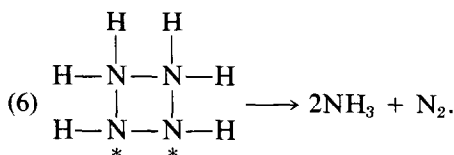
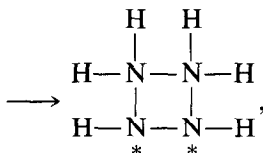
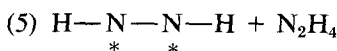
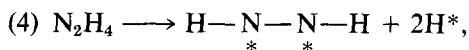
remains intact must be involved in the formation of nitrogen from hydrazine at room temperature. A hydrogen-abstraction step, involving two molecules of hydrazine in an activated complex, originally postulated by Szwarc (17), may be invoked here.

A suggested mechanism involves two modes for the catalytic decomposition of hydrazine. In one mode, hydrazine dissociatively adsorbs on iridium (perhaps only on certain crystalline faces, as has been suggested (1,2) for the case of  $\text{W}$  and  $\text{Mo}$  surfaces) degrading rapidly to  $\text{NH}^*$  radicals, nitrogen adatoms, and hydrogen adatoms.

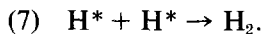
- (1)  $\text{N}_2\text{H}_4 \rightarrow 2\text{NH}_2^*$ ,
- (2)  $\text{NH}_2^* \rightarrow \text{NH}^* + \text{H}^*$ ,
- (3)  $\text{NH}^* \rightarrow \text{N}^*(\beta) + \text{H}^*$ .

In the other mode, hydrazine molecules chemisorb by way of hydrogen abstraction and by way of subsequent interaction with

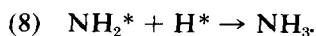
another hydrazine molecule from the vapor phase to form ammonia and nitrogen:



Molecular hydrogen is formed by recombination of the highly mobile hydrogen adatoms:



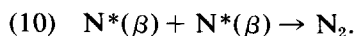
Steps 4–7 account for the product stoichiometry observed at temperatures up to about 500 K (Fig. 5). They also provide a pathway to  $\text{N}_2$  that preserves the integrity of the N–N bond in the parent hydrazine molecule. In the temperature range 500–600 K, larger ammonia/hydrogen and ammonia/nitrogen ratios are observed (Fig. 5), which suggest that the rate of an ammonia-forming reaction such as step 8 becomes significant:



At temperatures greater than 600 K, ammonia formation virtually ceases, while  $\text{N}_2$  and  $\text{H}_2$  are produced by way of steps 7 and 9:



Desorption of nitrogen adatoms in the  $\beta$ -state (step 10) requires temperatures greater than 900 K (Fig. 2):

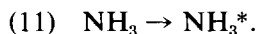


The  $\alpha$ -nitrogen peak observed in the de-

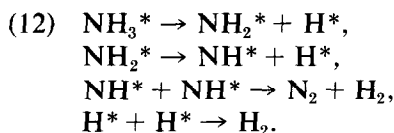
sorption spectra (Figs. 2 and 3) more than likely comes from physisorbed  $\text{N}_2$  formed in step 6.

The strongly bound  $\beta$ -nitrogen gradually preempts sites on which hydrazine adsorption can occur, thus causing a diminution in overall catalytic activity from that observed with the freshly cleaned surface (Fig. 4).

In contrast to the rapid room temperature decomposition of hydrazine on iridium, ammonia is quite stable and simply chemisorbs on the metal surface in a molecular state:



At about 600 K, however, the ammonia admolecules rapidly decompose to hydrogen and nitrogen, which appear in the gas phase.



The suggested decomposition pathway provides no means for the population of the nitrogen  $\beta$ -state, which is consistent with the experimental observations.

The energy separation between the states of the various adsorbed species provides us with a tool for evaluation of the catalytic effect of each state. Long exposure of the iridium to hydrazine ( $> 1$  hr at  $P \sim 10^{-7}$  Torr) resulted in a surface with greatly diminished catalytic activity (Fig. 8). Starting with such a surface, populated with all the species observed during programmed desorption, we selectively and sequentially removed individual species by heating for about 3-min intervals to successively higher temperatures. In the periods between heating, the activity of the catalyst was tested by passage of  $\text{N}_2\text{H}_4$  through the reactor with concurrent measurement of the surviving fraction of  $\text{N}_2\text{H}_4$  in the reactor effluent. The results (Fig. 8) indicate that removal of



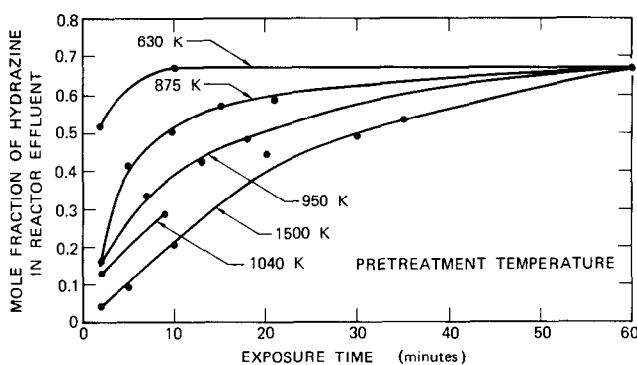


FIG. 8. Fraction of hydrazine in reactor effluent as a function of exposure time and of pretreatment temperature of catalyst. *P* reactor:  $\sim 10^{-7}$  Torr.

species that desorb rapidly below 630 K (ammonia,  $\alpha$ -nitrogen, and  $\alpha$ -hydrogen) does not restore the original high catalytic activity. However, removal of  $\beta$ -nitrogen restores high activity (Fig. 8). Additional evidence for the role of  $N^*(\beta)$  in the loss of catalytic activity is implied in the observed increase in the population of this state with hydrazine exposure (Fig. 3).

These results were supplemented by experiments in which the effect of preadsorbed hydrogen on the rate of hydrazine decomposition was evaluated. The iridium ribbon was first cleaned by heating under vacuum to 1500 K, then given an exposure of 300 Langmuirs to molecular hydrogen at 300 K. This exposure produced a coverage of  $8 \times 10^{14}$  H-atoms/cm<sup>2</sup> on the Ir surface, as measured from the H<sub>2</sub> desorption peak. Subsequent exposure of the hydrogen-pretreated catalyst to hydrazine demonstrated higher initial activity than observed for a clean Ir surface (Fig. 4). In addition, the mole fraction of NH<sub>3</sub> in the reactor effluent was notably higher at the expense of that of H<sub>2</sub>, while the mole fraction of N<sub>2</sub> was essentially unaffected in comparison to the case for the freshly cleaned Ir surface (Fig. 4). These data suggest that a minor route to NH<sub>3</sub> exists (other than that shown in step 6). We postulate a path such as step 8 to be a significant source of NH<sub>3</sub> at temperatures in the

range 500–700 K (Fig. 5), in addition to being the source of the NH<sub>3</sub> peak observed during desorption (Fig. 2).

In consequence of the importance of  $\beta$ -nitrogen with regard to the catalytic activity of the iridium surface, we made a careful measurement of the activation energy for desorption,  $E(N_\beta)$ , from this

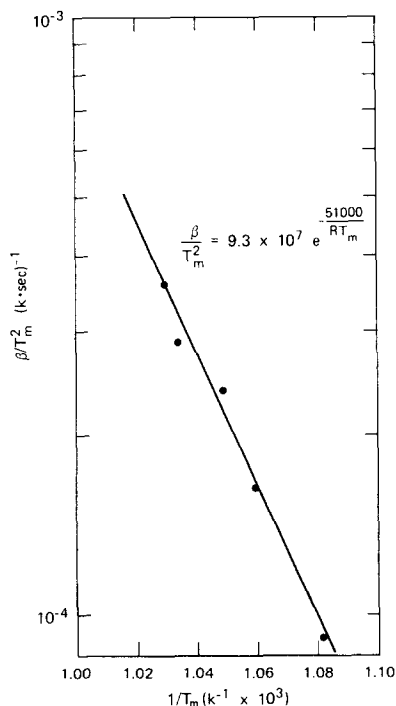


FIG. 9.  $\log(\beta/T_m^2)$  as a function of  $1/T_m$  for desorption of  $\beta$ -nitrogen.

state. From our analysis of the thermal desorption curves obtained at different heating rates, we compute  $E(N_\beta) = 51$  kcal/mole (Fig. 9). The preexponential constant for the desorption process is found to be  $A = 1.1 \times 10^{-2}$  cm<sup>2</sup> sec<sup>-1</sup>. In accordance with absolute rate theory (18), this value represents an entropy change of 48 e.u. for the transition between the bound state and the activated complex. An entropy change of this magnitude is indicative of associative desorption of atoms from a relatively immobile layer.

The persistence of  $\beta$ -nitrogen on the iridium surface after exposure to N<sub>2</sub>H<sub>4</sub> was verified by examination of the catalyst with Auger electron spectroscopy (AES). The iridium ribbon was exposed to hydrazine vapor until a marked reduction in catalytic activity was observed (Fig. 8). The reactor was then backfilled and the ribbon was transferred to the AES vacuum system. A low beam current ( $< 5$   $\mu$ A) was used to reduce the possibility of electron-induced desorption. After a spectrum from the "poisoned" catalyst was recorded, the ribbon was heated to successively higher temperatures, and spectra were recorded during the cool intervals between heatings. The results show that the AES signal due to nitrogen on the iridium surface does not significantly diminish in intensity until temperatures around 1000 K are attained, in agreement with the desorption spectra.

Our results point to an important characteristic inherent in Ir, namely, the strong surface bonding of nitrogen atoms produced during the N<sub>2</sub>H<sub>4</sub> decomposition. Possibly, the gradual accumulation of N\*( $\beta$ ) or the formation of a nitridic surface structure on the catalyst contributes to catalyst deactivation.

## ACKNOWLEDGMENTS

We are grateful to our colleagues Drs. John Falconer, David Golden, and Sidney W. Benson for discussions of the results.

## REFERENCES

1. Cosser, R. C., and Tompkins, F. C., *Trans. Faraday Soc.* **67**, 526 (1971).
2. Contaminard, R. C. A., and Tompkins, F. C., *Trans. Faraday Soc.* **67**, 545 (1971).
3. Contour, J. P., and Pannetier, G., *J. Catal.* **24**, 434 (1972).
4. Escard, J., Leclere, C., and Contour, J. P., *J. Catal.* **29**, 31 (1973).
5. Mimeault, V. J., and Hansen, R. S., *J. Phys. Chem.* **70**, 3001 (1966).
6. Mimeault, V. J., and Hansen, R. S., *J. Chem. Phys.* **45**, 2240 (1966).
7. Guthrie, A., and Wakerling, R. K., "Vacuum Equipment and Techniques," pp. 35ff. McGraw-Hill, New York, 1949.
8. Baker, B. R., and Wood, B. J., *J. Vac. Sci. Technol.* **8**, 555 (1971).
9. Redhead, P. A., *Vacuum* **12**, 203 (1962).
10. Gundry, P. M., and Tompkins, F. C., *Quart. Rev.* **1960**, 257; Ehrlich, G., and Hudda, F. G., *Phil. Mag.* **8**, 1587 (1963).
11. Chen, R., *Surface Sci.* **43**, 657 (1974); Falconer, J. L., and Madix, R. J., *Surface Sci.* **48**, 393 (1975).
12. Golden, D. M., Solly, R. K., Gac, N. A., and Benson, S. W., *J. Amer. Chem. Soc.* **94**, 363 (1972).
13. Benson, S. W., and O'Neal, H. E., "Kinetic Data on Gas Phase Unimolecular Reactions," NSRDS-NBS-21, U.S. Govt. Printing Office, Washington, DC, 1969.
14. Kant, A., and McMahon, W. J., *J. Inorg. Nucl. Chem.* **15**, 305 (1960).
15. Block, J., and Schultz-Erkloff, G., *J. Catal.* **30**, 327 (1973).
16. Sayer, C. F., Tech. Report 69/10, Rocket Propulsion Establishment, Westcott, England, 1969.
17. Szwarc, M., *Proc. Roy. Soc., Ser. A* **198**, 267 (1949).
18. Glasstone, S., Laidler, K. J., and Eyring, H., "The Theory of Rate Processes," Chap. 7. McGraw-Hill, New York, 1941.